Amino-ether macrocycle that forms Cu^{II} templated threaded heteroleptic complexes: A detailed selectivity, structural and theoretical investigations

Saikat Santra, Sandip Mukherjee, Somnath Bej, Subrata Saha and Pradyut Ghosh*

Department of Inorganic Chemistry, Indian Association for the Cultivation of Science, 2A & 2B Raja S. C. Mullick Road, Kolkata 700032, India. E-mail: icpg@iacs.res.in

_____

Abstract

A new oxy(ether)tris(amine) macrocycle, **MC** has been synthesized for Cu^{II} complex formation within the cavity of the macrocyclic wheel in endotopic fashion. This complex is further reacted with the bidentate chelating ligands, 1,10-phenanthroline (**L1**), 2,2′-bipyridyl (**L2**), 4,4′-dimethyl-2,2′-bipyridyl (**L3**) and 5,5′-dimethyl-2,2′-bipyridyl (**L4**) to achieve the pseudorotaxanes **PRT1**-**PRT4** respectively. These bis-heteroleptic complexes are characterized by the electrospray ionization mass spectrometry (ESI-MS), UV/Vis, EPR spectroscopy and Single-crystal X-ray structural analysis. Binding constants of the heteroleptic complexes are found in the range of 1.16×10^2 to 1.55×10^3 M^{-1} in acetonitrile. Further, the double level selectivity studies of **MC** using different metal ions [Co^{II}, Ni^{II}, Cu^{II}, Zn^{II}] and a number of simple bidentate chelating ligands shows the selective formation of **PRT1** that justifies the self-sorting nature of the system. Further, substitution of axles from pseudorotaxanes **PRT2**-**PRT4** could also be achieved by **L1** with nearly 100% efficiency. To corroborate the experimental studies

(comparison with the crystal geometry, importance of the π-π stacking etc.) the geometries of the pseudorotaxanes are optimized using DFT (B3LYP) in gas phase.

Introduction

Metal-ligand coordination bonding driven heteroleptic self-assembly has been developed as a popular strategy for constructing supramolecular multidimensional architectures with various physicochemical properties.[1] In recent time, organic macrocyclic ligands with centrally directed metal ion binding sites such as pyridyl ring,[2] imine,[3] amine,[4] sulfide,[5] phosphine,[6] oxy ether,[7] azacrown ether[8] etc. have shown potential application in the area of recognition,[9] sensing,[4,10] catalysis,[11] self-assemblies[7(b),12] and so on. Moreover, heteroleptic metal complexes by using such macrocyclic metal ion complexes have been successfully utilized for the development of interlocked molecular systems like pseudorotaxanes,[13] rotaxanes[1(c),13(c),14] and catenanes.[15] In this direction, Sauvage[16] and Leigh[2(c),17] have extensively exploited Cu^I and Pd^{II} towards the synthesis of a large number of mononuclear/multinuclear threaded systems. Judicious incorporation of chemical functionalities in the ligand backbone brings interesting properties such as selectivity and self-sorting in such metallo supramolecular assemblies.[18] Several examples of self-sorting by thoughtful choice of ligands, involving different numbers of metal-ion binding sites are reported in the literature for the formation of various metallo supramolecular architectures.[18(b,d,f)] This property also brings interesting features in metal templated interlocked molecular systems.[19] In other direction, Stoddart *et al* have extensively used electron deficient tetracationic macrocyclic wheel and electron-rich naphthyl,[20] tetrathiafulvene[21] and various electron rich organic guest molecules for the formation of host-guest assemblies.[22] We are currently interested on developing various threaded/interlocked

molecular systems composed of heteroditopic macrocyclic wheel, and the axle with multiple functionalities. In this direction, we have recently explored the template directed synthesis of [2] pseudorotaxanes and [2] rotaxanes by a bis(amido)tris(amine) functionalized macrocycle using the concept of metal templation as well as π stacking interactions.[23] It is worth mentioning that such macrocyclic wheel with amine and amide functionality in threaded systems is rare in the literature. To introduce another new combination of heteroditopic functionalities in the wheel component, it would be interesting to develop threaded structures with amino-ether based macrocycle. Here we report a new 27 membered tris(amino)oxy(ether) macrocycle, **MC** (Chart 1) and it's prospect towards the formation of different Cu^{II} templated threaded heteroleptic complexes using the concept of metal templation as well as π-stacking interaction and selectivity studies.

Results and discussion

Strategy and ligand designing aspects

Different types of strategies have been developed in recent decades for the formation of metal-based heteroleptic assemblies.[18(a),24] In general, (i) the subtle differences in ligand design, (ii) use of orthogonal recognition motifs, (iii) incorporation of suitable π-stacking units, (iv) use of steric constrains, (v) metal ion coordination number or (vi) metal ion oxidation states are the convenient ways to incorporate the selectivity and sorting nature of heteroleptic metallo-supramolecular systems. Our aim is to design a suitable macrocyclic host, capable of forming the metal ion templated heteroleptic complexes and the multi component systems that can show selectivity and self-sorting property. In brief, our designing strategies focus on the following aspects: (i) macrocyclic receptor having secondary amine moieties is our choice as the amine

functionality present in the macrocycles are suitable for metal ion coordination, (ii) incorporation

of 'V'- shaped aryl 1,2-diol functionality to rigidify the macrocyclic system, (iii) two aromatic

rings adjacent to the metal coordinating site via a benzyl spacer are attached because it is

expected that the presence of the aromatic spacers in the macrocyclic ligands would contributes

to its rigidity. Further, this could interact through π–π stacking with the pyridyl units of the axle

molecules (**L1-L4**) (Chart 1) favoring the heteroleptic aggregation, (iv) cleft with ethereal and

amine functionality in the ligand backbone are used to obtain the heteroditopic nature of the

wheel.

General procedure for the synthesis of macrocycle and Cu^{II} complexes

Scheme 1 shows the synthesis of **MC** in three steps. Reaction of 4-hydroxybenzaldehyde with

excess 1,2-dibromoethane in presence of anhydrous K_2CO_3 in acetonitrile at 80°C results the

compound **I**.

Chart 1. *Chemical Structures of* oxy(ether)tris(amine) *Macrocycle (**MC**) and bidentate chelating*

*ligands (**L1 – L4**)*
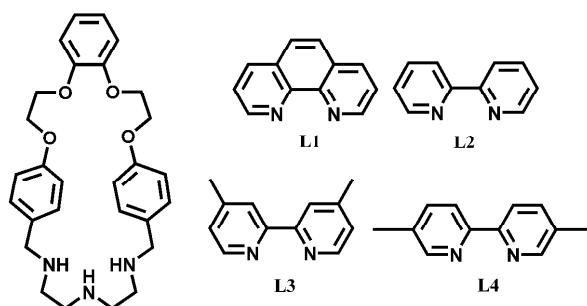
Scheme 1. *Synthetic route for preparation of **II** and **MC**.*ᵃ
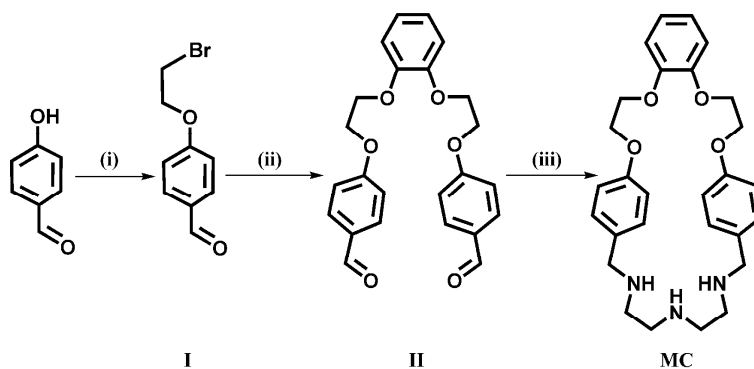
a *(i) 1,2-Dibromoethane, K$_2$CO$_3$, acetonitrile, reflux 82% ; (ii) Catechol, K$_2$CO$_3$, DMF, reflux, 85% ; (iii) Diethylenetriamine, Chloroform, Methanol, NaBH$_4$, 73%.*

Compound **II** is obtained upon reaction between catechol and compound **I** at 100°C in dry DMF in presence of anhydrous K$_2$CO$_3$ as base. High dilution reaction between diethylenetriamine and **II** in DCM/methanol (drop-wise addition) followed by reduction with NaBH$_4$ at room temperature results in the desired macrocyclic host **MC**. All the compounds are characterized by usual spectroscopic methods. [(**MC**)Cu^{II}(ClO$_4$)$_2$] and complex could be readily synthesized by reaction between equimolar amounts of the macrocycle and Cu^{II} salt in DCM/methanol (Scheme 1S, ESI). Heteroleptic ternary complexes are prepared in high yields by the reaction of the **MC**-Cu^{II} complex with bidentate chelating ligands **L1-L4** (Scheme 2S, ESI). The detailed synthetic procedures and characterization data are presented in experimental section.

UV/Vis and EPR studies

UV/Vis spectroscopy is used to explore the efficiency of the newly synthesized macrocyclic wheel (**MC**) towards pseudorotaxane formation. At room temperature, the UV/Vis spectrum of the tridentate macrocyclic ligand with equimolar amount of Cu^{II} shows λ$_{max}$ at ~ 630 nm (ε = 128.9 M^{-1} cm^{-1}) in methanol corresponds to d-d transition (Fig. 12S, ESI). Binding affinity of this newly synthesized tris-chelating wheel, **MC**, towards Cu^{II} is monitored *via* UV/Vis titration

experiments in methanol. Upon increasing the amount of the metal ion to the solution of macrocyclic wheel during titration, a gradual increase of absorption peak intensity at ~ 630 nm is observed up to one equivalent of metal ion (Fig.14S, ESI). Sigmoidal-curve fit analysis indicates the 1:1 binding stoichiometry between **MC** and metal ion (Fig.14S, ESI). The UV/Vis titration data shows the best fit for 1:1 model and association constants, K_a is obtained as 1.91 x 10^2 M^{-1} by Benesi-Hildebrand plot analysis[25] (Fig. 14S, ESI). Then the **MC**-Cu^{II} complex is allowed to evaluate their efficacy towards pseudorotaxane formation by reacting with bidentate chelating ligands **L1-L4**. Upon addition of various bidentate chelating ligands (**L1-L4**) separately to the acetonitrile solution of **MC**-Cu^{II} complex, gradual red shifts of the absorption bands are observed (Fig. 15S, ESI). The d-d bands obtained in the region 600-680 nm are the characteristic peaks of five coordinated Cu^{II} complexes.[26] This five coordinated square pyramidal or trigonal bipyramidal geometry around the Cu^{II} center could only be achieved if tridentate wheel and bidentate axle binds to the metal ion in a '3+2' orthogonal mode within the cavity of **MC**. Thus, the absorption maxima values are also in good agreement to prove the five coordinated heteroleptic complex formation. UV/Vis titration experiments are carried out to confirm the ternary complex formation by individual addition of **L1-L4** in to the solution of **MC**-Cu^{II} complex (1 mM) in acetonitrile. **MC**-Cu^{II} complex shows an absorption maxima 605 nm in acetonitrile (Fig.13S, ESI). Upon increasing the amount of guest ligands, the optical density of the metallo-macrocycle complex at 605 nm gradually decreases with concomitant generations of a new absorption maxima peak at 676, 680, 668 and 674 nm for **PRT1**, **PRT2**, **PRT3** and **PRT4** respectively (Fig. 1 (a), (c) and Fig. 18S, 21S, ESI). Upon consumption of one equivalent of each of the chelating bidentate ligands (**L1-L4**), saturation points are observed which confirms the 1:1 stoichiometric binding pattern towards ternary complex formation. The inflection points obtained

from the equivalent plot analysis further indicate the 1:1 stoichiometry between host metal complexes with guest ligands (Fig. 1 (b), (d) and Fig. 19S, 22S, ESI). Clear and single isosbestic points obtained during titration experiments reveal the existence of a single equilibrium in each case. The association constants of all the threaded complexes are calculated as K_a 1.55 x 10^3, 1.70 x 10^2, 1.84 x 10^2 and 1.16 x 10^2 M^{-1} respectively in acetonitrile, by using the Benesi-Hildebrand plot analysis (Fig. 16S, 17S, 20S and 23S in ESI). The λ_{max} values of the threaded ternary complexes, molar extinction coefficient values, association constants and free energy changes are tabulated below (Table 1).
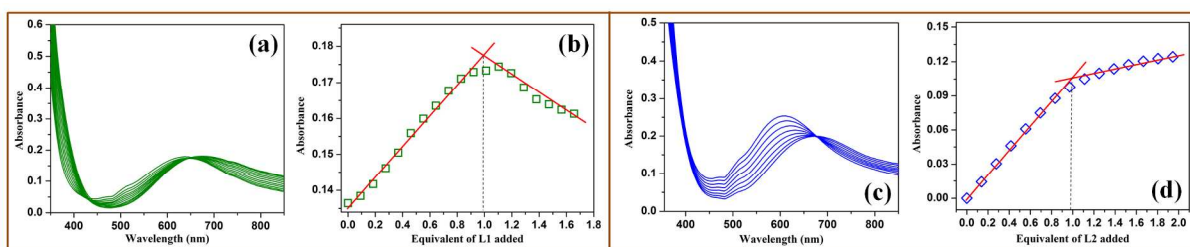
Fig. 1 *UV/Vis titration profile of (a)* ***MC****-Cu^{II} complex (1.0 × 10^{-3} M) with the aliquots of* ***L1*** *(1.2 × 10^{-2} M) (c)* ***MC****-Cu^{II} complex (9.0 × 10^{-4}M) with aliquots of* ***L2*** *(1.25 × 10^{-2} M) in acetonitrile. Selected UV/Vis spectra are shown for clarity whereas equivalent plots show more points. (b) and (d) shows equivalent plot from the data obtained via UV/Vis titration.*

Table 1. *UV/Vis Spectroscopic details for threading of* ***L1-L4*** *to the* ***MC****-Cu^{II} complex*

Axles	λ_{max}(nm)	Molar Extinction Coefficient (ε) (M^{-1} cm^{-1})	Association Constant [a] (K_a) (M^{-1})	Free Energy Change(Δ G°) [kcal/mol]
L1	676	1.72 x 10^2	1.55 x 10^3	- 4.38
L2	680	1.73 x 10^2	1.67 x 10^2	- 3.01
L3	668	1.83 x 10^2	1.84 x 10^2	- 3.11
L4	674	1.85 x 10^2	1.16 x 10^2	- 2.83

[a] Errors are calculated within 20%
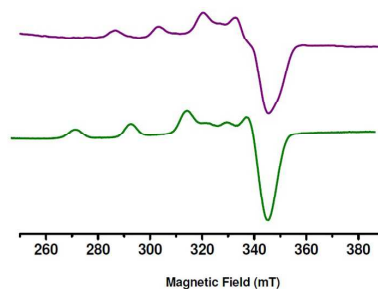
*Fig. 2 X-Band EPR spectra of **PRT1** (violet) and **PRT2** (green) in acetonitrile at 80 K.*

Additionally, the X-band EPR spectra of **PRT1** - **PRT4** show the patterns with $g_{II} > g\perp$ (Table 2), which indicate that the unpaired electron is localized in a d_{x2-y2} orbital of the Cu^{II} center, providing the penta-coordination environment with a distorted square pyramidal geometric arrangement around the Cu^{II} in the macrocyclic cavity of **MC** (Fig. 2 and Fig. 24S, 25S, ESI).

Table 2. $g_{II,}$ $g_{\perp}$ values obtained from X-Band EPR spectrum

Complex	g_{II}	$g_{\perp}$
PRT1	2.19133	1.91262
PRT2	2.19594	2.00655
PRT3	2.20351	2.02803
PRT4	2.20236	2.02235

ESI-MS Studies: The ESI-MS data of **MC**-Cu^{II}·$2ClO_4^-$ shows a molecular ion peak at $m/z =$ 639.1 (Fig. 3) with an isotopic distribution pattern consistent with the presence of a single copper ion within the cavity of **MC**. The peak at 639.1 appears due to $[(MC)(Cu^{II})(ClO_4)]^+$ species.
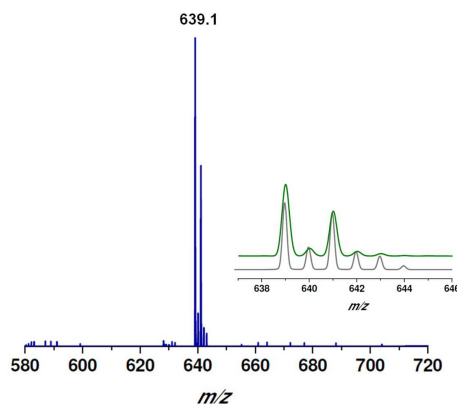
Fig. 3 *Mass (+ESI mode) spectra of the* $[(\mathbf{MC})(Cu^{II})(ClO_4)]^+$. *The inset picture depicts the enlarged portion in the region for the corresponding mono-positive ion (Green Colored) and their isotopic distribution pattern (Gray Colored).*

Formation of ternary complexes is monitored by using both perchlorate (ClO_4^-) (Fig. 4a, 4c, 4d and Fig 26S, 28S, 30S, 32S, ESI) and triflate (OTf^-) counter anion (Fig. 4b and Fig 27S, 29S, 31S and 33S) of **MC**-Cu^{II} complex. For threaded complexes **PRT1** to **PRT4**, the peaks observed in the ESI-MS data clearly reveals the existence of such complexes in gaseous phase. In Fig. 4 the prominent peaks seen at *m/z* 819.17, 845.2, 823.23, 823.25 for the corresponding monopositive ions indicate the formation of heteroleptic complexes between **MC**, Cu^{II} and
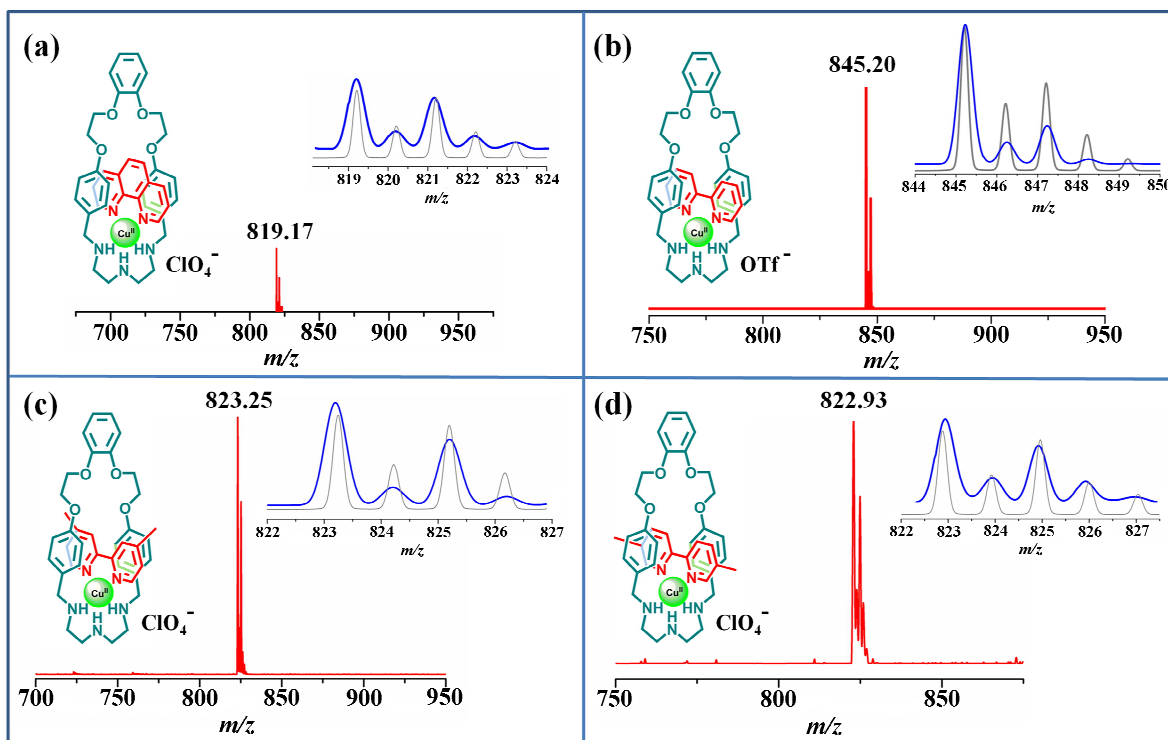
Fig. 4 *Mass (+ESI mode) spectra of the [2] pseudorotaxanes. (a), (c) and (d) show peaks for* ***PRT1***, ***PRT3*** *and* ***PRT4*** *with one* ClO_4^- *counter anion and (b) shows peak for* ***PRT2*** *with* OTf^- *counter anion. The inset picture depicts the enlarged portion in the region for the corresponding mono-positive ion (Blue Colored) and their isotopic distribution pattern (Gray Colored).*

corresponding chelating ligands **L1-L4**. Further a peak at m/z = 639.1 $[(MC)(Cu^{II})(ClO_4)]^+$ is observed (Fig. 26S, 28S, 30S, 32S, ESI) which could be attributed for the complexes after losing the corresponding chelating ligands. In every cases, isotopic distribution show good agreement of the desired ternary complex formation (Fig. 4).

Single crystal X-ray structural analysis

Fig. 5 shows the single crystal X-ray structures of the five metal complexes. Structural analysis shows that the coordination sphere of the metal center of **MC**-Cu^{II} $[\{(MC)Cu^{II}(CH_3CN)_2\}\cdot(ClO_4)_2]$ is occupied by five nitrogen atoms (bond distances ranges from 1.963 to

2.292 Å, Table 1S) with the square pyramidal geometry. The basal plane of the distorted square pyramidal Cu^{II} center is occupied by the three nitrogen donor atoms N1, N2 and N3 of **MC** and N4 of solvent molecule (acetonitrile); whereas the apical position is taken up by N5 from another acetonitrile molecule. Thus, Cu^{II} is coordinated in endotopic fashion in the cavity of **MC** with two coordinated solvent molecules. The cavity dimensions of the MC unit can be described by the length, measuring 12.623 Å (measured as the distance from the centroid of the upper benzene ring to N2 in the **MC**-Cu^{II} complex) and the width, measuring 5.829 Å (measured as the distance of the two centroids of the two benzene rings on the side-arms of the macrocycle in the **MC**-Cu^{II} complex). In **MC**-Cu^{II}, this cavity is occupied by one acetonitrile molecule ligated to the basal plane of the Cu^{II} center, while the other acetonitrile molecule protrudes outside. This cavity is exploited to bind bidentate chelating ligands (**L1-L4**) with the Cu^{II} center of **MC**-Cu^{II} upon replacing solvent molecules to achieve the heteroleptic assemblies (**PRT1-PRT4**). Single crystal X-ray structures of the pseudorotaxanes also confirm penta coordinated Cu^{II} centers for these complexes. The space-filling model of ternary complexes **PRT1** [{(**MC**)Cu^{II}(**L1**)}·(PF$_6$)$_2$], **PRT2** [{(**MC**)Cu^{II}(**L2**)}·(ClO$_4$)$_2$]**,** and **PRT4** [{(**MC**)Cu^{II}(**L4**)}·(PF$_6$)$_2$·DMF] show complete threading of **L1**, **L2** and **L4** inside the macrocyclic cavity of **MC**, whereas **L3** showed partial threading in case of **PRT3** [{(**MC**)Cu^{II}(**L3**)}·(ClO$_4$)$_2$]. The observed π–π stacking interacting distances in all the ternary complexes between two parallel arene moieties of **MC** and the pyridyl unit of bidentate chelating ligands are consistent with the expectations.[23(a,c)] These interactions are one of the major factors towards high yield synthesis of heteroleptic aggregation over other homoleptic alternatives.

In the structure of **PRT3**, we find that two different units (**A** and **B**) of the complex are present in the asymmetric unit (Fig. 5). The geometrical parameters for the two units differ very slightly.

The coordination geometry of the unit **B** is closer to the trigonal bipyramidal structure (see later). In both the units, threading is incomplete, or in other words the aromatic stacking is not as effective as in the other complexes. Therefore, the coordination geometry may be expected to be more fluxional (in solution) in the square pyramid to trigonal bipyramid spectrum.

The coordination geometries of the five copper complexes make an interesting reading. In the five coordinated systems the τ value is generally used to characterize the geometries relative to the two ideal geometries, square pyramidal (with τ value of 0) and trigonal bipyramidal (with τ value of 1).[27] In the **MC-Cu^{II}** complex the copper ion is in an almost purely square pyramidal geometry (with a τ value of 0.0983). But, upon threading of the axles (**L1-L4**) the coordination geometries are changed significantly (due to steric constraints, π-π interaction and the fixed lower bite angle of the ligands of around 80°). Compared to the square pyramidal complex **MC-Cu^{II}**, the complex **PRT4** has τ value of 0.9567, implying almost ideal trigonal bipyramidal geometry. However, **PRT1** (τ = 0.5397), **PRT2** (τ = 0.6363) and unit **A** of **PRT3** (τ = 0.5687) are at the middle of the geometrical spectrum, while the unit **B** of **PRT3** (τ = 0.8058) structure has shifted more towards the trigonal bipyramidal geometry. Cu–N bond distances, τ value, and π–π stacking distances of **PRT1**, **PRT2**, **PRT3** and **PRT4** are summarized in Table 3.

Crystal structure reveals that the two adjacent arene moiety of **MC-Cu^{II}** are not at all parallel, which is expected because there is no possibility of aromatic π-stacking at such high distances. Upon threading of the axles (**L1-L4**), π-π stacking becomes operative between the arene moieties of the wheel and electron deficient axle molecules. Compared to the **MC-Cu^{II}** structure the cavity dimensions are somewhat modified in the threaded complexes due to the incorporation of the aromatic ligands (**L1-L4**). The lengths have been reduced to about 12.3-12.4 Å and the widths have been increased to about 6.5 Å (to accommodate the threaded ligands).
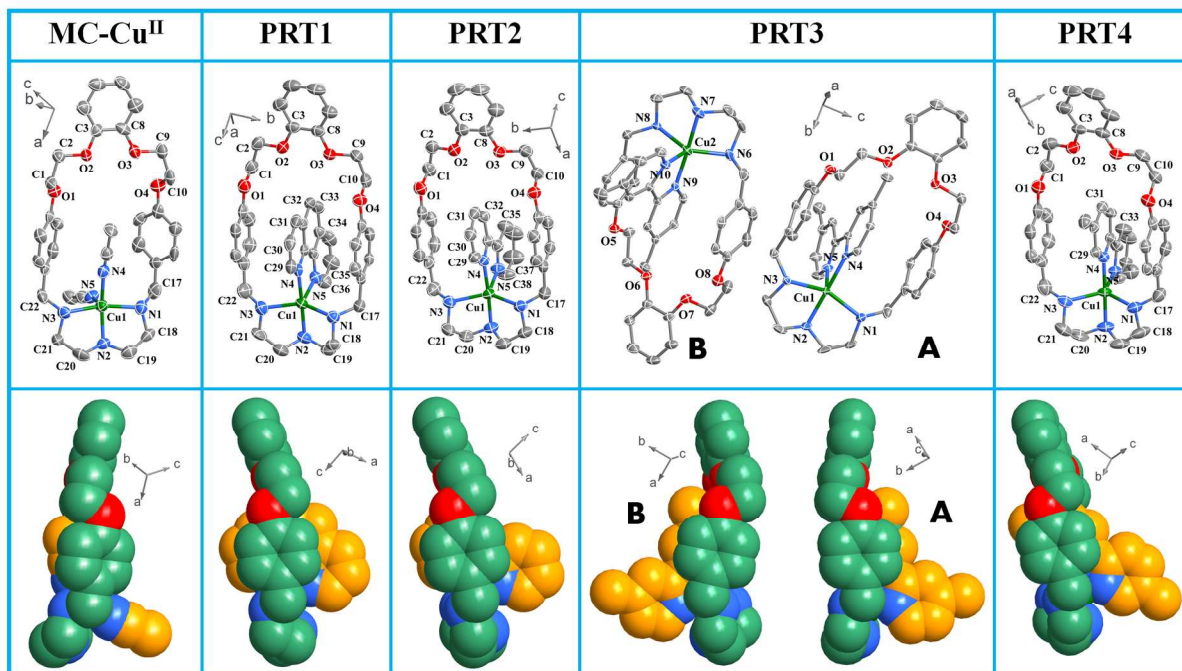
*Fig. 5 (Top) Thermal ellipsoid probability plots of the basic units of **MC-Cu^{II}** and **PRT1-PRT4**. Hydrogen atoms, solvent molecules and anions have been removed for clarity. Thermal ellipsoids are at the 40 % probability level. (Bottom) Spacefill diagrams of the threaded ternary complexes.*

Table 3. Important structural parameters for **MC-Cu^{II}** and **PRT1-PRT4**.

Complex	Cu–N[a] [Å]	τ value[b]	π–π stacking[c] [Å]
MC-Cu^{II}	1.963-2.292	0.0983	-
PRT1	1.994-2.137	0.5397	3.411-3.385
PRT2	2.014-2.154	0.6363	3.435-3.417
PRT3	1.989-2.169 (A)	0.5687 (A)	3.359-3.450 (A)
	1.985-2.183 (B)	0.8058 (B)	3.462-3.328 (B)
PRT4	1.978-2.169	0.9567	3.379-3.375

*[a] The lowest and highest values of the Cu–N bond lengths, [b] τ calculated from the crystal structures of **PRT1-PRT4**. [c] Distances between the centroids of the arene moieties of **MC** and the pyridyl (nearest) unit of the axles.*

Table 4. Crystallographic Data and Refinement Parameters for **MC-Cu^{II}** and **PRT1-PRT4**.

	MC-CuII.2ClO$_4$	PRT1.2PF$_6$	PRT2.2ClO$_4$	PRT3.2ClO$_4$	PRT4.2PF$_6$
empirical formula	C$_{32}$H$_{41}$N$_5$O$_{12}$Cl$_2$Cu	C$_{40}$H$_{43}$N$_5$O$_4$F$_{12}$P$_2$Cu	C$_{38}$H$_{43}$N$_5$O$_{12}$Cl$_2$Cu	C$_{40}$H$_{47}$N$_5$O$_{12}$Cl$_2$Cu	C$_{43}$H$_{54}$N$_6$O$_5$F$_{12}$P$_2$Cu
Fw	822.15	1011.27	896.21	924.26	1088.40
T (K)	150(2)	150(2)	150(2)	150(2)	150(2)
crystal system	monoclinic	monoclinic	monoclinic	triclinic	monoclinic
space group	$P2_1/c$	$P2_1/c$	$P2_1/c$	$P-1$	$P2_1/n$
a/Å	25.141(3)	19.500(6)	19.9719(17)	15.7961(6)	13.316(4)
b/Å	9.0132(11)	10.305(3)	10.4277(9)	16.1332(6)	26.117(9)
c/Å	16.941(2)	24.405(7)	22.0793(19)	18.3202(7)	13.810(5)
α/deg	90.00	90.00	90.00	86.435(1)	90.00
β/deg	104.205(4)	105.740(8)	103.675(2)	84.547(1)	97.715(10)
γ/deg	90.00	90.00	90.00	84.769(1)	90.00
V/Å^3	3721.6(8)	4721(2)	4467.9(7)	4621.5(3)	4759(3)
Z	4	4	4	4	4
ρ_{calcd} (g cm^{-3})	1.4673	1.4229	1.3324	1.3284	1.5190
μ (Mo Kα) (mm^{-1})	0.7973	0.6213	0.6704	0.6503	0.6242
λ/Å	0.71073	0.71073	0.71073	0.71073	0.71073
F (000)	1708	2068	1860	1924	2244
collected reflns	23860	40432	50980	59645	28888
unique reflns	3147	5606	7612	17854	3701
GOF (F^2)	1.152	1.057	1.100	1.091	1.072
R_1[a]	0.0790	0.0530	0.0588	0.0581	0.0767
wR_2[b]	0.2275	0.1430	0.1662	0.1456	0.2046

[a]$R_1 = \Sigma ||F_o| - |F_c|| / \Sigma |F_o|$, [b]$wR_2 = [\Sigma\{w(F_o^2 - F_c^2)^2\}/\Sigma\{w(F_o^2)^2\}]^{1/2}$.

14

The π-π stacking interaction distances are tabulated in Table 3. Depending upon the steric encoding and rigidity present in the organic guest molecules, selectivity and different kind of threading are observed in the threaded heteroleptic complexes.

Selectivity and self-sorting studies

In metallo-supramolecular assembled structures, self-sorting is controlled by various factors; such as, metal-ligand coordination, π-π interactions, steric and other electronic effects.[18(c,e,f)] Upon mixing of all the components (**MC**, bidentate chelating ligands, and divalent metal ions), at equilibrium the reaction mixture do not afford a statistical mixture of all possible combinations of ternary complexes in solution. Instead, only a multicomponent assembled structure is isolated from the reaction mixture which showed the preference towards Cu^{II} templated **L1** threaded heteroleptic complexation. To investigate the selectivity and self-sorting properties of the newly synthesized macrocycles with different divalent transition metal ion and chelating ligands, we have carried out three steps selectivity study by using ESI-MS and UV/Vis spectroscopic technique. Detailed procedure for the solution state selectivity study and isolation of the self-sorted complexes are discussed in experimental section.

Self-sorting in MC-Cu^{II} complex and bidentate chelating ligands: To inspect the electronic, steric, pi-pi stacking and maximum site occupancy upon threading inside the cavity of metal-macrocycle complex, the combination of four bidentate chelating ligands (**L1-L4**) are chosen (Chart 1). Upon mixing of one equivalent **MC**, Cu^{II} and each of the bidentate ligands **L1-L4** in DCM/methanol, threaded heteroleptic complexes like **PRT1-PRT4** and other homoleptic aggregation between the axle molecules are expected. Such kind of multiple combinations are

reduced to only one complex formation that is revealed by ESI-MS and UV/Vis spectroscopic tools. ESI-MS study shows the selective formation of **PRT1**. A single charged species at *m/z* 819.1 along with the **MC**-Cu^{II} complex (*m/z* = 639.1) is observed [Fig. 43S (b) in ESI]. ESI-MS peak at *m/z* = 639.1 is obtained due to dethreading of the axle component during mass spectometric analysis. No peaks of the (**L2-L4**) threaded heteroleptic aggregation in the ESI-MS study are detected. Isolated green colour complex also shows the characteristic peaks of the **PRT1** in UV-Vis study in acetonitrile [Fig. 43S (a) in ESI]. The selective formation of the heteroleptic complex over the homoleptic aggregation could be due to the suitable π-π stacking interaction between the arene moieties present in the macrocyclic wheel and chelating ligands. Such kind of interaction renders heteroleptic aggregation over the homoleptic complexes.

All the other combinations of the heteroleptic threaded complexes having π-π stacking interactions should show up with more or less probability. But in solution selectively signature of **L1** threaded heteroleptic complex is observed. This could be due to suitable pi stacking upon threading and restricted rotation around C-C bond in the ligand compared to other bipyridyl derivative (**L2-L4**). UV/Vis titration experiment and Benesi-Hildebrand plot analysis reveal that the **L1** threaded pseudorotaxane shows highest association constant among **L1-L4** (Table 1).

As the phenanthroline **L1** shows higher selectivity over bipyridyl derivatives (**L2 – L4**), we have further explored a phenanthroline derivative, **L5** (neocuproine) for threading and selectivity studies (Chart 1S, ESI). Elemental analysis, ESI-MS (Fig. 34S, 35S, ESI) and UV/Vis (Fig. 36S, ESI) studies do not support the exclusive formation of **L5** threaded heteroleptic complex in stoicheometric amount. This could be due to the steric effect exerted by the methyl group pointed towards the metal coordinating sites upon threading. Thus, from this experiment it is revealed

that both ligand structure (phenanthroline vs bipyrydyl derivatives) and steric crowding exerted by the substitution play crucial roles for the selective formation of a heteroleptic complex.

Templated metal ion selectivity of MC towards threaded complex formation: The metal ion selectivity study is carried out upon mixing of one equivalent of **MC**, **L1** and each of the divalent transition metal ions Co^{II}, Ni^{II}, Cu^{II}, Zn^{II} (one equivalent of each) in DCM/methanol. This experiment shows the selective formation of Cu^{II} templated threaded complex due to the suitable geometry ('3+2' donor sets) provided by the bidentate chelating orthogonal motifs and macrocyclic wheel to Cu^{II} center. Further, ESI-MS study of the resulting solution mixture and UV/Vis spectrum of the isolated green complex support the formation of **PRT1** [Fig.44S (a) and 44S (b) in ESI].

Self-sorting studies: Complexation upon mixing of perchlorate salts of four divalent metal ions (Co^{II}, Ni^{II}, Cu^{II}, Zn^{II}), guest ligands L1-L5 and newly synthesized wheel MC: Equimolar amounts of tri-dentate wheel (**MC**), four divalent transition metal ions and five bidentate chelating guest ligands (**L1-L5**) are dissolved in DCM/methanol solution and are stirred for 3-4 hours. A greenish blue precipitate is formed, which is isolated and characterized by ESI-MS (Fig. 41S, ESI). Mass spectrometry data shows m/z at 819.2 corresponding to the [**PRT1**·ClO_4^-].

The absorption spectrum (Fig. 42S, ESI) of the isolated complex further supports the selective formation of **PRT1.** This reveals the selectivity of such system towards **L1** threaded, Cu^{II} pseudorotaxane structure by tridentate wheel **MC** among possible twenty threaded heteroleptic complexes.

The degree of self sorting for mononuclear assemblies M equals to P_0/P where P_0 indicates the number of all probable combinations and P specify the number of all actual number of

assemblies formed in the experiment.[28] Thus, higher value of M pointing towards the lesser number of the products formed in the experiment and hence higher degree of self sorting. In this experiment, 20 such possibilities of threaded heteroleptic complex formation may possible. But the self sorted and selected formation of **PRT1** ruled out other ternary complex formation, suggesting higher degree of self sorting having a value M = 20.

Ligand substitution studies: Ligand substitution, external stimuli dependent tunable molecular aggregation and assembly/disassembly studies in the interlocked architectures bring interesting properties in the threaded host guest complexes.[23(b),29] As the selectivity study showed preference of **MC-Cu**[II] complex towards **L1**, we have carried out the ligand substitution reaction between **L1** and isolated threaded complexes **PRT1-PRT4**. De-threading processes are monitored via UV/Vis spectroscopic technique (Scheme 3; Fig. 6 and Fig. 37S (a) in ESI).

Scheme 2. *Selectivity towards one heteroleptic complex, PRT1 over other possibilities*
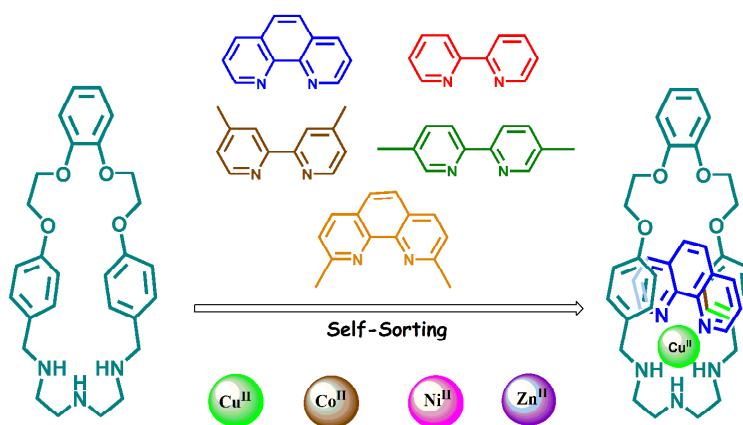
As shown in Fig. 6(a) and Fig. 6(b), a gradual shift of the absorption bands is observed when the solution of **L1** is added to the solution of **PRT2-PRT3**. Upon saturation, new peaks are

generated at 676 nm in each case which corresponds to the absorption peak of **PRT1** in acetonitrile. A clear isosbestic point in all the titration studies indicates the complete transformation of **PRT2-PRT4** to **PRT1** via single equilibrium process. The detailed characteristic peaks (λ_{max}) of the parent ternary complexes and newly generated peak corresponds to **PRT1** tabulated below (Table 5). After ligand exchange, the resulting solutions are subjected to ESI-MS analysis. In the ESI-MS spectra (Fig. 38S-40S, ESI), no noticeable characteristic peaks of **PRT2**-**PRT4** are observed and a prominent characteristic peak of **PRT1** is observed in each case, indicating the good selectivity of **L1** over **L2**, **L3** or **L4** towards heteroleptic complex formation. To further demonstrate the selectivity of **L1** towards heteroleptic complex formation, we have also isolated the green crystalline materials of **PRT1** by adding equivalent amount of **L1** to the respective solutions of **PRT2-PRT4**. The green crystalline complexes are characterized by elemental analysis, UV/Vis, ESI-MS and EPR spectroscopy. These data matched well with the data obtained from the analysis of **PRT1**.

Scheme 3.

PRT2 : R$_1$ = R$_2$ = H
PRT3 : R$_1$ = CH$_3$, R$_2$ = H
PRT4 : R$_1$ = H, R$_2$ = CH$_3$

PRT1
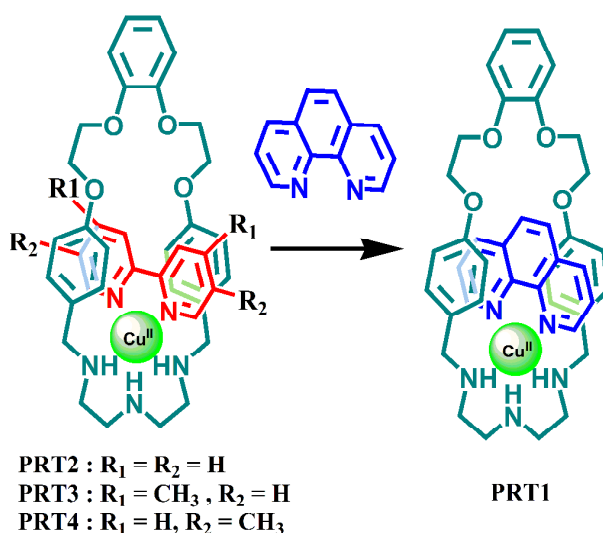
Table 5. *Data of the parent absorption peaks of respective complexes (**PRT2-PRT4**), final absorption peaks obtained upon axle substitution by **L1** via de-threading.*

Complex[a]	Parent Absorption Peak (nm)	Final Absorption Peak at Saturation Point (nm)
PRT2	680.0	676.0
PRT3	662.0	676.0
PRT4	677.0	676.0

*[a] The titrations of **PRT2-PRT4** with **L1** were performed in acetonitrile.*
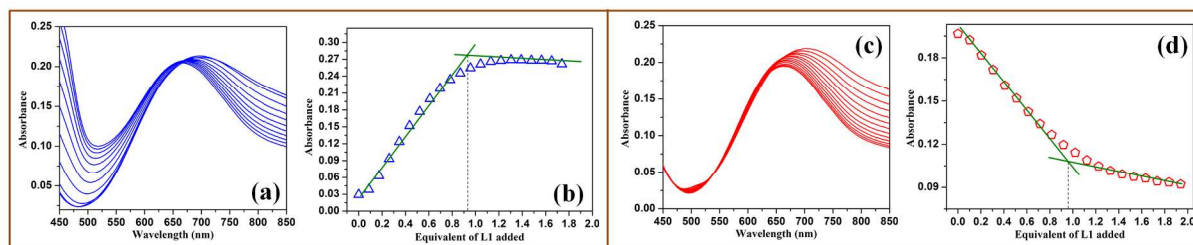
Fig.6 *UV/Vis titration profile for dethreading of (a) **L3** (1 × 10⁻³ M), and (c) **L4** (1 × 10⁻³ M) from corresponding [2]Pseudorotaxanes in presence of 1 × 10⁻² M Phenanthroline (**L1**) in acetonitrile. Selected UV/Vis spectra are shown for clarity whereas equivalent plots show more points.*

Theoretical study

To investigate the importance of the π-π stacking of the aromatic ligands with the two benzene rings on the macrocycle (**MC**), we used the conformation of the macrocycle from the **PRT1** (in which the faces of the benzene rings are arranged parallel to each other) geometry for calculating its optimized structure of **MC**. In the optimized geometry of **MC**, (Fig. 9) we can see that the two opposing benzene rings (in the side arms) are not at all parallel (in other words, they do not stack-up). In fact, this is also true for the structure of **MC**-Cu^{II} (crystal structure, Fig. 7). Therefore, the stacking of these two benzene rings is not necessary even for the simple complex formation. This stacking however is necessary for the stabilization (with respect to **MC**-Cu^{II}) of the bipyridyl and phenanthroline complexes (**PRT1-PRT4**). The distance between the centroids

of the two benzene rings in **MC** and **MC-Cu**^{II} are 5.56 (optimized) and 5.83 Å (crystal) respectively. For **PRT1-PRT4** the corresponding distances (6.53-6.72 Å for crystal geometries and 6.83-7.07 Å for the optimized geometries) are increased from this value to accommodate the second aromatic ligand. This conformation change is just right for an effective π-π stacking of three aromatic rings at a favourable separation (~3.5 Å). This fact is further supported form the study of the optimization steps from the **MC** geometry corresponding to **PRT1** to its lowest energy conformation (Fig. 8). The final optimized geometry of **MC** (Conf. III in Fig. 8) is about 25.6 kcal/mol energetically favourable compared to the conformation of **MC** obtained (Conf. I in Fig. 8) from the geometry of the complex **PRT1** (by removing the metal-ion and the ligand **L1**).

The geometries of **PRT1-PRT4** are optimized to see the similarities or differences in their crystal structures and vacuum structures (which provide better models for the solution phase structures). From the analysis of the optimized geometries it is evident that compared to their crystal geometries all of the complexes have slightly expanded coordination spheres (increased Cu-N distances; for example 0.06 Å in case of **PRT1**). This also resulted in the slight expansion of π-π stacking distances (0.15-0.20 Å). However, the stacking is expected to be still important and effective in the vacuum optimized geometries, as the relative positions of the aromatic faces have not changed and the faces are still parallel to each other.

MC	[(MC)Cu^{II}(MeCN)$_2$]	[(MC)Cu^{II}(Phen)]/PRT1
(optimized)	(crystal)	(crystal)
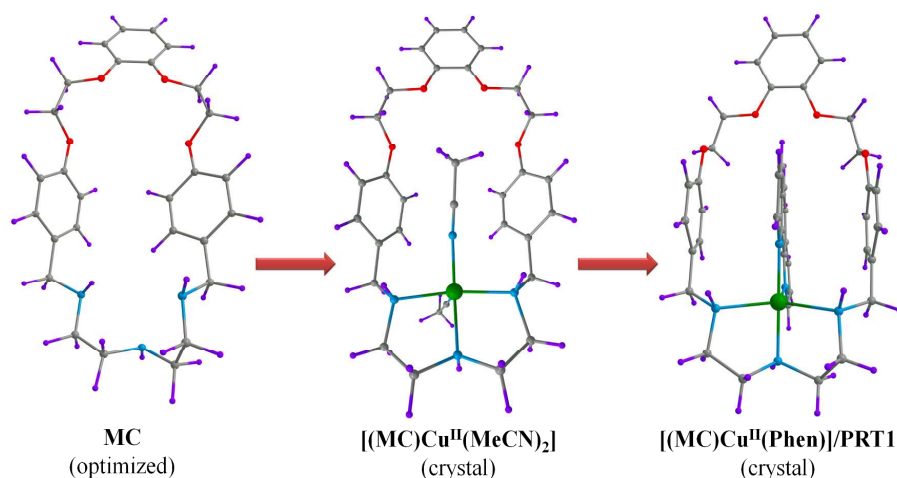
*Fig. 7 Comparison of the structures (perspective views) of the **MC** (optimized structure) as a free molecule and in two complexed forms, showing the orientation of the opposite benzene rings.*

As the coordination geometries for the Cu^{II} in **PRT1** and **PRT2** resemble more closely to the square pyramidal (SP) geometry it is expected that the unpaired electron should reside in the $d_{(x^2-y^2)}$ orbital (which is confirmed from the EPR studies). The spin density maps and Mulliken spin density values for the coordinated nitrogen atoms provide evidence in favor of this fact (Fig. 9 and Fig. 45S-47S in ESI). The coordination geometries of the complexes **PRT3** and **PRT4** resemble more closely to trigonal bipyramidal (TBP), however best described as having a mixed geometry (tending more towards TBP rather than SP). In such cases, the unpaired electron on the Cu^{II} is expected to reside in an orbital best described by a linear combination of $d_{(x^2-y^2)}$ and d_{z^2} orbitals. The shapes of the spin density maps and the Mulliken spin density values on the copper ions and the coordinated nitrogen atoms also support this conclusion (Table 2S, ESI).
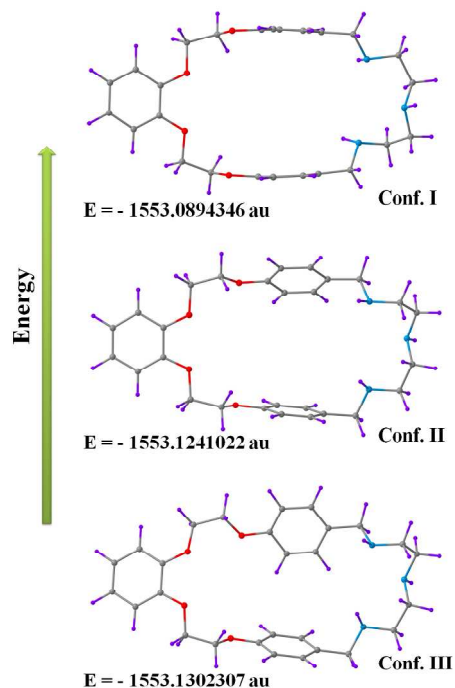
Fig. 8 *Comparison of the energies of three conformations in the course of optimization of the structure of **MC**. **Conformation III** is the final optimized structure and **Conformation I** is the initial structure (used as the starting geometry for the optimization) obtained from the crystal structure geometry of **PRT1**. **Conformation II** is a randomly selected intermediate geometry.*

Crystal Structure   **Optimized Structure**

(a)

(b)

(c)

(d)

Distance(Å)	Crystal	Optimized
A-B	3.385	3.655
B-C	3.411	3.557
A-C	6.542	6.983
N2-D	12.348	12.391
Cu-N1	2.140	2.220
Cu-N2	1.997	2.076
Cu-N3	2.138	2.178
Cu-N4	2.000	2.027
Cu-N5	2.115	2.192
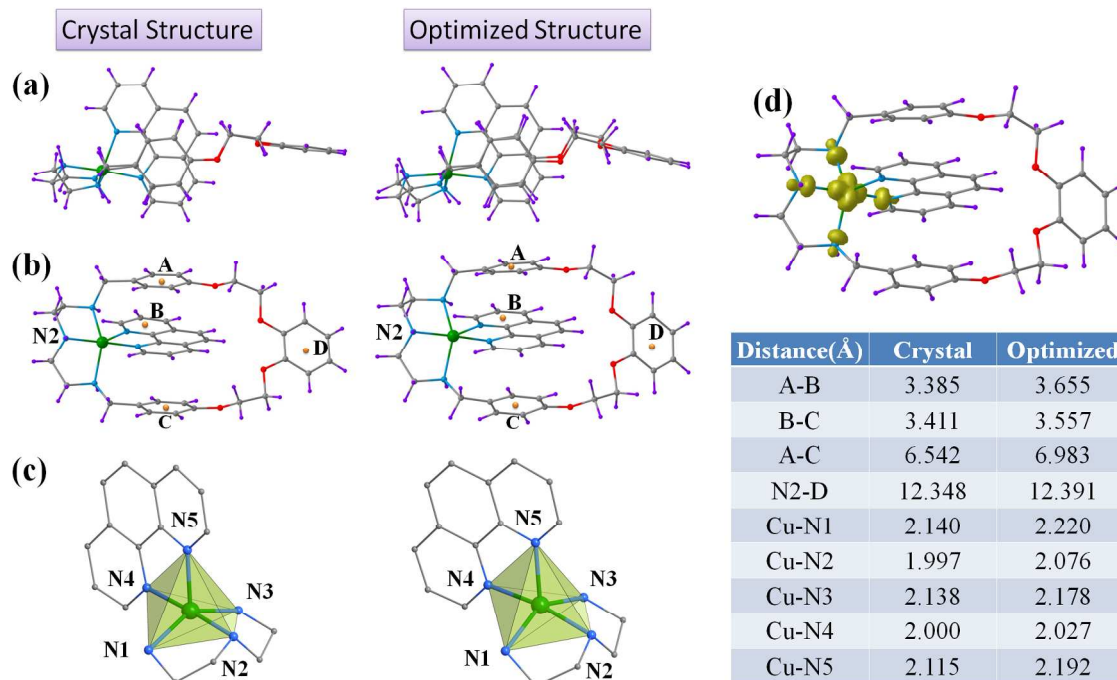
*Fig. 9 Comparison between the crystal structure and the optimized structure for **PRT1** [Color Code: Green, Cu; Blue, N; Gray, C; Purple, H; Red, O; Orange, Centroid]. (a) Structural view perpendicular to the π-π stacking planes, (b) Structural view showing the centroids of the aromatic rings used for measuring important stacking distances, (c) View highlighting the coordination sphere of the copper ion, (d) Spin density map obtained from the analysis of the optimized structure showing that the unpaired electron resides in the $d_{(x2-y2)}$ orbital (supporting the experimental EPR results) of the Cu^{II} ion with the roughly square pyramidal geometry. The isodensity surfaces correspond to a value of 0.01 e/b^3.*

Conclusion

In summary, we have developed a new macrocycle with heteroditopic binding units such as tris-amine and oxy-ether. The tris(amine)oxy(ether) functionalized macrocycle has shown it's potentiality for the high-yield syntheses of metal ion templated heteroleptic threaded complexes with different bidentate chelating ligands. This tris-amino macrocycle shows selectivity and self-

sorting properties towards the formation of a heteroleptic aggregation over twenty such possibilities from the mixture of ten components (one macrocyclic wheel, five bidentate chelating ligands and four divalent transition metal ions). Metal ion binding sites, $\pi-\pi$ stacking interactions, geometrical arrangement around the metal center, steric crowding influence the selectivity of such heteroleptic aggregation. Substitution of chelating ligands from the self assembled structures by stronger bidentate chelating ligands is achieved with about 100% efficiency. This strategy could be utilized towards the formation of a variety of interlocked systems with complex functionalities. We are presently exploring various entrenched functionalities in such heteroleptic threaded complexes by utilising the heteroditopic nature present in the wheel and ligand substitution strategy.

Experimental section

Materials and methods

All reactions were carried out in argon gas atmosphere followed by workup at ambient conditions. $Cu(ClO_4)_2 \cdot 6H_2O$, $Ni(ClO_4)_2 \cdot 6H_2O$, $Co(ClO_4)_2 \cdot 6H_2O$, $Zn(ClO_4)_2 \cdot 6H_2O$ $Cu(CF_3SO_3)_2$, KPF_6, deuterated solvents, 1,10-phenanthroline, 2,2′-bipyridyl, 4,4′-dimethyl-2,2′-bipyridyl, 5,5′-dimethyl-2,2′-bipyridyl, 2,9-dimethyl-1,10-phenanthroline, diethylenetriamine, 4-hydroxybenzaldehyde were purchased from Sigma-Aldrich and were used as received. DCM, Chloroform, DMF, 1,2-dibromoethane, potassium carbonate were purchased from Spectrochem Pvt. Ltd., India. Acetonitrile, methanol, DCM and DMF were dried via convenient procedures and were collected over molecular sieve before use.

High-resolution mass spectrometry (HRMS) analysis was performed on QToF−Micro YA 263 Mass spectrometer in positive ESI mode. ^1H, ^{13}C, experiments were carried out on FT-NMR

Bruker DPX 300/400 MHz NMR spectrometer. The absorption studies were performed in a PerkinElmer Lambda 900 UV−vis−NIR spectrometer (NIR = near-infrared) (with a quartz cuvette of path length 1 cm). Elemental analysis was performed on PerkinElmer 2500 series II elemental analyzer, PerkinElmer, USA. Chemical shifts for ^{1}H and ^{13}C NMR were reported in parts per million (ppm), calibrated to the residual solvent peak set, with coupling constants reported in Hertz (Hz).

Synthesis of compound I

4-hydroxybenzaldehyde (122 mg, 1 mmol) is treated with excess 1,2-dibromoethane (215 µL, 2.5 mmol) in presence of K_2CO_3 (400 mg, 3 mmol) and the reaction mixture is refluxed for 24 hours using acetonitrile as solvent under nitrogen atmosphere. Then the reaction mixture is evaporated to dryness under *vaccuo* and extracted using chloroform and water. The organic layer is repeatedly washed with brine and the yellow semi-solid product is purified by column chromatography using 94:6 hexane and ethyl acetate respectively. The white crystalline product is isolated and characterized. Yield ~82%. All characterisation data matches well with the literature values[30]. ^{1}H NMR (400 MHz, $CDCl_3$): δ (ppm) 4.45 (s, 4H, - CH_2), 7.05 (d, 2H, *J* = 8 Hz, Ar-*H*), 7.85 (d, 2H, *J* = 8 Hz, Ar-*H*), 9.91 (s, 1H, Ar-*CHO*). ^{13}C NMR (75 MHz, $CDCl_3$): δ (ppm) 28.7, 67.9, 114.8, 130.4, 131.9, 130.3, 162.9, 190.6.

Synthesis of compound II

Compound **I** (480 mg, 2.1 mmol) is reacted with catechol (110 mg, 1 mmol) in DMF in presence of anhydrous K_2CO_3 (400 mg, 3 mmol) and the reaction mixture is refluxed for 2 days under nitrogen atmosphere at 100°C. Then the reaction mixture is poured into ice cold water and the white precipitate obtained is collected by filtration. Yield: 342 mg (~85 %). ESI-MS (+ve): m/z

calculated for $C_{12}H_{10}N_8Na$ [M + Na]$^+$ 429.14 , Found 429. 30. ^{1}H NMR (400 MHz, CDCl$_3$): δ

(ppm) 4.38 (s, 8H, - *CH$_2$*), 6.99-7.02 (m, 8H, Ar-*H*), 7.79 (d, 4H, *J* = 8 Hz, Ar-*H*), 9.86 (s, 2H,

Ar-*CHO*). ^{13}C NMR (75 MHz, CDCl$_3$): δ (ppm) 67.1, 68.1, 115.0, 115.8, 122.5, 130.3, 132.1,

149.0, 163.8, 190.8. DEPT-135 NMR (75 MHz, CDCl$_3$): 67.0, 68.0, 114.9, 115.7, 122.4, 131.9,

190.7. Anal. Calcd for $C_{24}H_{22}O_6$: C, 70.92; H, 5.46. Found: C, 70.81; H, 5.39.

Synthesis of compound MC

In a 500 mL three neck round bottom flask, two are fitted with 100 mL pressure equalizer and

another for nitrogen atmosphere. Compound **II**, (406 mg, 1.0 mmol) in 50 mL DCM in a

pressure equalizer and diethylenetriamine (0.1 mL, 1.0 mmol) dissolved in 50 mL of DCM in

another pressure equalizer, were added drop by drop to the stirring 100 mL methanol solvent.

After complete addition, the reaction mixture is stirred for 12h. Sodium borohydride 76 mg (2

mmol) is added to the reaction mixture and stirred for 3h. The reaction mixture is filtered and the

filtrate is evaporated. The solid is dissolved in 100 mL of DCM and washed with water and brine

solution. The organic phase is separated, and dried over anhydrous sodium sulphate. The solvent

is evaporated in *vaccuo* to yield the desired product **MC** as white solid.Yield: 353 mg (~73 %).

ESI-MS (+ve): *m/z* calculated for $C_{28}H_{35}N_3O_4$ [M+H]$^+$ 478.59, Found 478.31. ^{1}H NMR (400

MHz, CDCl$_3$): δ (ppm) 2.79-2.87 (m, 8H, - *CH$_2$*), 3.68 (s , 4H, - *CH$_2$*) ,4.29 - 4.35 (m, 8H, -*CH$_2$*),

6.78 (d, 4H, J = 8Hz, Ar-*H*), 6.98 - 6.99 (m, 4H, Ar-*H*), 7.14 (d, 4H, J = 8Hz, Ar-*H*).). ^{13}C NMR

(75 MHz, CDCl$_3$): δ (ppm) 67.1, 68.1, 115.0, 115.8, 122.5, 130.3, 132.1, 149.0, 163.8, 190.8.

DEPT-135 NMR (75 MHz, CDCl$_3$): 48.2, 48.7, 53.3, 67.3, 69.0, 114.8, 116.1, 122.4, 129.4.

Anal. Calcd for $C_{28}H_{35}N_3O_4$: C, 70.42; H, 7.39; N, 8.80. Found: C, 70.51; H, 7.43; N, 8.89.

Synthesis of complex (MC)Cu^{II}(ClO$_4$)$_2$

MC (0.1 mmol, 47.7 mg) is dissolved in 10 mL of methanol/DCM (1:1); Cu(ClO$_4$)$_2$·6H$_2$O (0.1 mmol, 37 mg) is added to the stirring solution. The reaction mixture is stirred for another 4h. A bluish precipitate is developed which is filtered and isolated after repeated washing with methanol. Characterized by elemental analysis, ESI mass spectrometry and UV/Vis spectroscopy [The complex was crystallized from an acetonitrile solution as {(MC)Cu^{II}(CH$_3$CN)$_2$}(ClO$_4$)$_2$]. Yield ~84%. λ_{max} = 630 nm in methanol, Molar Extinction Coefficient value in methanol (ε) 128.9 M^{-1} cm^{-1}, λ_{max} = 605 nm in acetonitrile, Molar Extinction Coefficient value in acetonitrile (ε) 266.67 M^{-1} cm^{-1}, ESI-MS: C$_{28}$H$_{35}$ClCuN$_3$O$_8$, 639.14; Found, 639.12. Anal. Calcd for C$_{32}$H$_{41}$Cl$_2$CuN$_5$O$_{12}$: C, 46.75; H, 5.03; N, 8.52. Found: C, 46.83; H, 5.11; N, 8.48.

Synthesis of [2] pseudorotaxanes

A solution of **MC** (0.1 mmol) and Cu(ClO$_4$)$_2$·6H$_2$O (0.1 mmol) in methanol (5 mL) is stirred for 10 minutes and the resultant mixture is added to the 0.1 mmol solution of each bidentate chelating ligand (**L1/L2/L3/L4**) separately for the formation of heteroleptic complexes **PRT1–PRT4** respectively. The resultant mixture is stirred for 3 h and the precipitate is collected by filtration and characterized by ESI mass, EPR spectroscopy, single crystal X-ray structural analysis (**PRT1-PRT4**). Yield of the crystalline product 78-85%.

The pseudorotaxanes are also prepared in the triflate (OTf$^-$) form, following the same procedure.

(a) Characterization of **PRT1**·(ClO$_4$)$_2$. λ_{max} = 676 nm in acetonitrile, Molar Extinction Coefficient value in Acetonitrile (ε) = 1.72 × 10^2 M^{-1} cm^{-1}, ESI-MS (+ve): *m/z* calculated for C$_{40}$H$_{43}$ClCuN$_5$O$_8$ [**PRT1**·ClO$_4$]$^+$ 819.21, Found 819.20. Anal. Calcd for C$_{40}$H$_{43}$Cl$_2$CuN$_5$O$_{12}$: C, 52.21; H, 4.71; N, 7.61. Found: C, 52.47; H, 4.68; N, 7.57.

(b) Characterization of **PRT2**·$(ClO_4)_2$. λ_{max} = 680 nm in acetonitrile, Molar Extinction Coefficient value in Acetonitrile (ε) = 1.71 x 10^2 M^{-1} cm^{-1}, ESI-MS (+ve): *m/z* calculated for $C_{38}H_{43}ClCuN_5O_8$ [**PRT2**·ClO_4]$^+$ 795.21, Found 795.45. Anal. Calcd for $C_{38}H_{43}Cl_2CuN_5O_{12}$: C, 50.93; H, 4.84; N, 7.81. Found: C, 50.86; H, 4.75; N, 7.74.

(c) Characterization of **PRT3**·$(ClO_4)_2$. λ_{max} = 668 nm in acetonitrile, Molar Extinction Coefficient value in Acetonitrile (ε) = 1.83 x 10^2 M^{-1} cm^{-1}, ESI-MS (+ve): *m/z* calculated for $C_{40}H_{47}ClCuN_5O_8$ [**PRT3**·ClO_4]$^+$ 823.24, Found 823.21. Anal. Calcd for $C_{40}H_{47}Cl_2CuN_5O_{12}$: C, 51.98; H, 5.13; N, 7.58. Found: C, 52.08; H, 5.24; N, 7.62.

(d) Characterization of **PRT4**·$(ClO_4)_2$. λ_{max} = 674 nm in acetonitrile, Molar Extinction Coefficient value in Acetonitrile (ε) = 1.85 x 10^2 M^{-1} cm^{-1}, ESI-MS (+ve): *m/z* calculated for $C_{40}H_{47}ClCuN_5O_8$ [**PRT4**·ClO_4]$^+$ 822.93, Found 823.21. Anal. Calcd for $C_{40}H_{47}Cl_2CuN_5O_{12}$: C, 51.98; H, 5.13; N, 7.58. Found: C, 51.88; H, 5.09; N, 7.63.

Guest Ligands (L1-L4) Selectivity Studies: Guest ligand selectivity of **MC** is carried out by adding a solution of $Cu(ClO_4)_2$·$6H_2O$ (0.1 mmol, 37 mg) in methanol (5 mL) to a solution of macrocycle **MC** (0.1 mmol, 47.7 mg) in methanol/DCM (5 mL) at room temperature. After 10 minutes, a mixture of bidentate chelating ligands (**L1**, **L2**, **L3** and **L4**) each of 0.1 mmol in 5 mL methanol/DCM are added to the solution. The mixture is stirred for 4 h. A greenish precipitate was formed which was filtered and the residue was washed with DCM and methanol. Then the green precipitate is collected and characterised by ESI-MS and UV/Vis spectroscopy which supports the formation of **PRT1**.

Templating metal ion selectivity experiment : **MC** (0.1 mmol, 47.7 mg) and **L1** (0.1 mmol, 19.6 mg) are dissolved in 10 ml methanol/DCM and stirred for 10 minutes, then a solution mixture of Co^{II}, Ni^{II}, Cu^{II}, Zn^{II} (0.1 mmol of each) in methanol (10 mL) is poured into the stirring solution at room temperature. After 4 h the greenish precipitate is collected by filtration and repeated wash with methanol. The precipitate is collected by filtration, dried and characterized by ESI-MS and UV/Vis spectroscopic tool.Both the characterization tool supports the formation of **L1** threaded heteroleptic complex, **PRT1**.

Selectivity study upon mixing of equimolar amount of tri-dentate wheel, four divalent transition metal ions (Cu^{II}, Co^{II}, Ni^{II}, Zn^{II}) and five (L1-L5) bidenatate chelating guest ligands: **MC** (0.1 mmol, 47.7 mg) and 0.1 mmol of each bidentate chelating ligands (**L1-L5**) are dissolved in methanol/DCM binary solvent mixture and allowed to stir at room temperature. Then a solution mixture containing 0.1mmol of each divalent transition metal ion (Co^{II}, Ni^{II}, Cu^{II}, Zn^{II}) in methanol is added to the stirring solution. The reaction mixtures are stirred for 3-4 hours. A greenish blue precipitate is developed which is filtered and washed several times with DCM and methanol. The precipitate is collected and analyzed by ESI-MS and UV/Vis spectroscopy. Mass spectrometry showed m/z at 819.2 corresponds to the **PRT1**·ClO_4^- .

Solution state selectivity study

Standard stock solutions of **MC** (1×10^{-3} M) in DCM, a mixture of **L1-L4** (1×10^{-3} M, each), a mixture of Cu^{II}, Zn^{II}, Ni^{II}, Co^{II} (1×10^{-3} M, each) in acetonitrile were prepared. i) For host ligand selectivity study, **MC** (1×10^{-3} M) and Cu^{II} (1×10^{-3} M) each of 50 µL were added in a glass vial

and then a solution containing **L1-L4** (1×10^{-3} M, each) 50 µL was added to the above mixture. The resulted clear solution was subjected for ESI-MS which showed the ternary complex peak corresponds to [**PRT1**·ClO$_4^-$]$^+$. ii) For templating metal ion selectivity, 50 µL of **L1** (1×10^{-3} M) and 50 µL of solution containing mixtures of Cu^{II} , Zn^{II} , Ni^{II} , Co^{II} (1×10^{-3} M, each) were mixed in a glass vial and then 50 µL of **L1** (1×10^{-3} M) was added to the above mixture. The resulted clear solution was subjected for ESI-MS which showed the ternary complex peak corresponds to [**PRT1**·ClO$_4^-$]$^+$. UV/Vis also supports the formation of **PRT1**(Fig.37S (b), ESI) iii) To achieve highest degree of self sorting, 50 µL of **MC** (1×10^{-3} M) and 50µL of solution containing mixtures of Cu^{II}, Zn^{II}, Ni^{II}, Co^{II} (1×10^{-3} M, each) were added in a glass vial and then a solution of **L1** –**L5** (1×10^{-3} M, each) 50 µL was added to the above mixture . The resulted clear solution was subjected for UV/Vis (Fig.37S (b), ESI) and ESI-MS which showed the ternary complex peak corresponds to [**PRT1**·ClO$_4^-$]$^+$.

Calculation of association constants

Associations between **MC** and Cu^{II} and metallo cycles with bidentate chelating ligands (**L1-L4**) were calculated using UV titration data. Association constants were calculated using Benesi−Hildebrand equation.

$1/(A-A_0) = 1/ \{(A_{max}-A_0) [Guest] K_a) \}+ 1/(A_{max}-A_0)$.

 A_0 is the absorbance of initial species taken in cuvette; A is the absorbances upon each addition of guest species. A_{max} is the absorbances at saturation point.

X-ray crystallographic data collection and refinements

Single crystal X-ray data for the five complexes, **MC-Cu**[II] and **PRT1-PRT4**, were collected on a Bruker SMART APEX CCD diffractometer using the SMART/SAINT software.[31] Intensity data were collected using graphite-monochromatized Mo Kα radiation (0.71073 Å) at 150 K. The structures were solved by direct methods using the SHELXL-2013[32] program incorporated into WinGX.[33] Empirical absorption corrections were applied with SADABS.[34] All non-hydrogen atoms were refined with anisotropic displacement coefficients. The hydrogen atoms bonded to carbon were included in geometric positions and given thermal parameters equivalent to 1.2 times those of the atom to which they were attached. Even though the data were collected at 150 K several times, we are unable to assign electron density for some solvent molecules in the unit cell. The SQUEEZE routine was applied to intensity data of **PRT1-PRT3** to take into account the solvent molecules. Crystallographic data and refinement parameters are given in Table 1.

Computational method

Full geometry optimizations through the Density Functional Theory (DFT), were carried out using the *Gaussian 09* package.[35] The optimizations were performed (for the purpose of comparison with the crystal geometries) using the hybrid B3LYP functional[36] as implemented in the *Gaussian 09* program. For the optimization of the structure of **MC**, the initial geometry was derived from the structure of **PRT1** (by removing **L1** and Cu[II]) and 631g(d) basis set was used for the calculation. The LanL2DZ basis set was used for all the atoms for **PRT1-PRT4**. Normal convergence criterion (10^{-4} a.u.) was applied for all the optimizations. The ground state geometry optimizations were monitored by the subsequent frequency test and no imaginary frequencies were observed.

Dalton Transactions Accepted Manuscript

Reference

1   (a) M. L. Saha, S. De, S. Pramanik and M. Schmittel, *Chem. Soc. Rev.*, 2013, **42**, 6860-6909; (b) R. Chakrabarty, P. S. Mukherjee and P. J. Stang, *Chem. Rev.*, 2011, **111**, 6810-6918; (c) J. E. Beves, B. A. Blight, C. J. Campbell, D. A. Leigh and R. T. McBurney, *Angew. Chem., Int. Ed.*, 2011, **50**, 9260-9327; (d) S. De, K. Mahata and M. Schmittel, *Chem. Soc. Rev.*, 2010, **39**, 1555-1575.

2   (a) A. Noor, S. C. Moratti and J. D. Crowley, *Chem. Sci.*, 2014, **5**, 4283-4290; (b) M. R. Halvagar and W. B. Tolman, *Inorg. Chem.*, 2013, **52**, 8306-8308; (c) A.-M. Fuller, D. A. Leigh, P. J. Lusby, I. D. H. Oswald, S. Parsons and D. B. Walker, *Angew. Chem., Int. Ed.*, 2004, **43**, 3914-3918; (d) R. J. Bordoli and S. M. Goldup, *J. Am. Chem. Soc.*, 2014,

136, 4817-4820; (e) J. Winn, A. Pinczewska and S. M. Goldup, *J. Am. Chem. Soc.*, 2013, **135**, 13318-13321.

3   (a) M. E. Belowich and J. F. Stoddart, *Chem. Soc. Rev.*, 2012, **41**, 2003-2024; (b) C. D. Meyer, C. S. Joiner and J. F. Stoddart, *Chem. Soc. Rev.*, 2007, **36**, 1705-1723.

4   M. Hu and G. Feng, *Chem. Commun.*, 2012, **48**, 6951-6953.

5   (a) M. Kadarkaraisamy and A. G. Sykes, *Polyhedron*, 2007, **26**, 1323-1330; (b) A. Tamayo, J. Casabo, L. Escriche, C. Lodeiro, B. Covelo, C. D. Brondino, R. Kivekaes and R. Sillampaeae, *Inorg. Chem.*, 2006, **45**, 1140-1149.

6   (a) R. Bigler, E. Otth and A. Mezzetti, *Organometallics*, 2014, **33**, 4086-4099; (b) M. T. Mock, S. Chen, M. O'Hagan, R. Rousseau, W. G. Dougherty, W. S. Kassel and R. M. Bullock, *J. Am. Chem. Soc.*, 2013, **135**, 11493-11496.

7   (a) S. K. Kim and J. L. Sessler, *Acc. Chem. Res.*, 2014, **47**, 2525-2536; (b) Y. Han, Z. Meng, Y.-X. Ma and C.-F. Chen, *Acc. Chem. Res.*, 2014, **47**, 2026-2040; (c) S. K. Kim, V. M. Lynch, N. J. Young, B. P. Hay, C.-H. Lee, J. S. Kim, B. A. Moyer and J. L. Sessler, *J. Am. Chem. Soc.*, 2012, **134**, 20837-20843.

8   T. Gunnlaugsson and J. P. Leonard, *Chem. Commun.*, 2003, 2424-2425.

9   (a) M. Boiocchi, M. Licchelli, M. Milani, A. Poggi and D. Sacchi, *Inorg. Chem.*, 2015, **54**, 47-58; (b) A. Kumar, S.-S. Sun and A. J. Lees, *Coord. Chem. Rev.*, 2008, **252**, 922-939.

10   M. M. Rhaman, F. R. Fronczek, D. R. Powell and M. A. Hossain, *Dalton Trans*, 2014, **43**, 4618-4621.

11   R. B. Hopkins and A. D. Hamilton, *J. Chem. Soc., Chem. Commun.*, 1987, 171-173.

12   (a) C. Browne, T. K. Ronson and J. R. Nitschke, *Angew. Chem., Int. Ed.*, 2014, **53**, 10701-10705; (b) L. F. Lindoy, K.-M. Park and S. S. Lee, *Chem. Soc. Rev.*, 2013, **42**, 1713-1727; (c) P. S. Mukherjee, N. Das, Y. K. Kryschenko, A. M. Arif and P. J. Stang, *J. Am. Chem. Soc.*, 2004, **126**, 2464-2473.

13   (a) K. A. McNitt, K. Parimal, A. I. Share, A. C. Fahrenbach, E. H. Witlicki, M. Pink, D. K. Bediako, C. L. Plaisier, N. Le, L. P. Heeringa, D. A. Vander Griend and A. H. Flood, *J. Am. Chem. Soc.*, 2009, **131**, 1305-1313; (b) J.-P. Collin, F. Durola, J. Frey, V. Heitz, J.-P. Sauvage, C. Tock and Y. Trolez, *Chem. Commun.*, 2009, 1706-1708; (c) J. D. Crowley, S. M. Goldup, A.-L. Lee, D. A. Leigh and R. T. McBurney, *Chem. Soc. Rev.*, 2009, **38**, 1530-1541.

14   (a) A. Joosten, Y. Trolez, J.-P. Collin, V. Heitz and J.-P. Sauvage, *J. Am. Chem. Soc.*, 2012, **134**, 1802-1809; (b) J.-P. Collin, S. Durot, M. Keller, J.-P. Sauvage, Y. Trolez, M. Cetina and K. Rissanen, *Chem. -Eur. J.*, 2011, **17**, 947-957; (c) B. Ventura, L. Flamigni,

J.-P. Collin, F. Durola, V. Heitz, F. Reviriego, J.-P. Sauvage and Y. Trolez, *Phys. Chem. Chem. Phys.*, 2012, **14**, 10589-10594.

15 (a) P. Mobian, J.-M. Kern and J.-P. Sauvage, *Inorg. Chem.*, 2003, **42**, 8633-8637; (b) C. Lincheneau, B. Jean-Denis and T. Gunnlaugsson, *Chem. Commun.*, 2014, **50**, 2857-2860; (c) K. D. Haenni and D. A. Leigh, *Chem. Soc. Rev.*, 2010, **39**, 1240-1251; (d) G. Kaiser, T. Jarrosson, S. Otto, Y.-F. Ng, A. D. Bond and J. K. M. Sanders, *Angew. Chem., Int. Ed.*, 2004, **43**, 1959-1962; (e) D. A. Leigh, P. J. Lusby, S. J. Teat, A. J. Wilson and J. K. Y. Wong, *Angew. Chem., Int. Ed.*, 2001, **40**, 1538-1543; (f) V. G. Schill, *Catenanes, Rotaxanes and Knots.* Academic Press, New York-London 1971; (g) V. Balzani, A. Credi, M. Venturi, *Molecular Devices and Machines: Concepts and Perspectives for the Nanoworld,* Second Edition, 2008.

16 (a) J.-P. Collin, C. Dietrich-Buchecker, P. Gavina, M. C. Jimenez-Molero and J.-P. Sauvage, *Acc. Chem. Res.*, 2001, **34**, 477-487; (b) M. Mohankumar, M. Holler, M. Schmitt, J.-P. Sauvage and J.-F. Nierengarten, *Chem. Commun.*, 2013, **49**, 1261-1263; (c) M. Mohankumar, M. Holler, J.-F. Nierengarten and J.-P.Sauvage, *Chem. -Eur. J.*, 2012, **18**, 12192-12195; (d) C. Roche, A. Sour and J.-P. Sauvage, *Chem. -Eur. J.*, 2012, **18**, 8366-8376; (e) J.-P. Sauvage, Y. Trolez, D. Canevet and M. Sallé, *Eur. J. Org. Chem.* 2011, 2413-2416.

17 (a) D. A. Leigh, P. J. Lusby, R. T. McBurney and M. D. Symes, *Chem. Commun.*, 2010, **46**, 2382-2384; (b) J. Berná, J. D. Crowley, S. M. Goldup, K. D. Hänni, A.-L. Lee and

D. A. Leigh, *Angew. Chem., Int. Ed.*, 2007, **46**, 5709-5713; (c) J. D. Crowley, K. D. Hanni, A.-L. Lee, D. A. Leigh, *J. Am. Chem. Soc.*, 2007, **129**, 12092-12093;

18   (a) X. Lu, X. Li, J.-L. Wang, C. N. Moorefield, C. Wesdemiotis and G. R. Newkome, *Chem. Commun.*, 2012, **48**, 9873-9875; (b) B. Brusilowskij, E. V. Dzyuba, R. W. Troff and C. A. Schalley, *Chem. Commun.*, 2011, **47**, 1830-1832; (c) M. Schmittel and K. Mahata, *Chem. Commun.*, 2010, **46**, 4163-4165; (d) M. Barboiu, F. Dumitru, Y.-M. Legrand, E. Petit and A. van der Lee, *Chem. Commun.*, 2009, 2192-2194; (e) K. Mahata and M. Schmittel, *J. Am. Chem. Soc.*, 2009, **131**, 16544-16554; (f) S. Ulrich and J.-M. Lehn, *J. Am. Chem. Soc.*, 2009, **131**, 5546-5559; (g) J.-M. Lehn, *Proc. Natl. Acad. Sci. U. S. A.*, 2002, **99**, 4763-4768.

19   K. Parimal, E. H. Witlicki and A. H. Flood, *Angew. Chem., Int. Ed.*, 2010, **49**, 4628-4632.

20   (a) C. J. Bruns, M. Frasconi, J. Iehl, K. J. Hartlieb, S. T. Schneebeli, C. Cheng, S. I. Stupp and J. F. Stoddart, *J. Am. Chem. Soc.*, 2014, **136**, 4714-4723; (b) S. Grunder, P. L. McGrier, A. C. Whalley, M. M. Boyle, C. Stern and J. F. Stoddart, *J. Am. Chem. Soc.*, 2013, **135**, 17691-17694.

21   T. Avellini, H. Li, A. Coskun, G. Barin, A. Trabolsi, A. N. Basuray, S. K. Dey, A. Credi, S. Silvi, J. F. Stoddart and M. Venturi, *Angew. Chem., Int. Ed.*, 2012, **51**, 1611-1615.

22   (a) M. Juricek, N. L. Strutt, J. C. Barnes, A. M. Butterfield, E. J. Dale, K. K. Baldridge, J. F. Stoddart and J. S. Siegel, *Nat. Chem.*, 2014, **6**, 222-228; (b) M. Juricek, J. C. Barnes,

N. L. Strutt, N. A. Vermeulen, K. C. Ghooray, E. J. Dale, P. R. McGonigal, A. K. Blackburn, A.-J. Avestro and J. F. Stoddart, *Chem. Sci.*, 2014, **5**, 2724-2731; (c) J. C. Barnes, M. Juricek, N. L. Strutt, M. Frasconi, S. Sampath, M. A. Giesener, P. L. McGrier, C. J. Bruns, C. L. Stern, A. A. Sarjeant and J. F. Stoddart, *J. Am. Chem. Soc.*, 2013, **135**, 183-192.

23   (a) S. Saha, I. Ravikumar and P. Ghosh, *Chem. Commun.*, 2011, **47**, 6272-6274; (b) S. Saha, I. Ravikumar and P. Ghosh, *Chem. - Eur. J.*, 2011, **17**, 13712-13719; (c) S. Saha, S. Santra and P. Ghosh, *Eur. J. Inorg. Chem.*, 2014, **2014**, 2029-2037; (d) S. Saha, S. Santra, B. Akhuli and P. Ghosh, *J. Org. Chem.*, 2014, **79**, 11170-11178.

24   M. L. Saha, S. Neogi and M. Schmittel, *Dalton Trans.*, 2014, **43**, 3815-3834.

25   B. Chowdhury, S. Khatua, R. Dutta, S. Chakraborty and P. Ghosh, *Inorg. Chem.*, 2014, **53**, 8061-8070.

26   G. A. McLachlan, G. D. Fallon, R. L. Martin and L. Spiccia, *Inorg. Chem.*, 1995, **34**, 254-261.

27   A. W. Addison, T. N. Rao, J. Reedijk, J. Van Rijn and G. C. Verschoor, *J. Chem. Soc., Dalton Trans.*, 1984, 1349-1356.

28   M. L. Saha and M. Schmittel, *Org. Biomol. Chem.*, 2012, **10**, 4651-4684.

29   (a) S. Sharma, G. J. E. Davidson and S. J. Loeb, *Chem. Commun.*, 2008, 582-584; (b) H. Zhang, Q. Wang, M. Liu, X. Ma and H. Tian, *Org. Lett.*, 2009, **11**, 3234-3237; (c) F. Huang, K. A. Switek and H. W. Gibson, *Chem. Commun.*, 2005, 3655-3657; (d) S. Saha and J. F. Stoddart, *Chem Soc Rev*, 2007, **36**, 77-92; (e) L. Zhu, H. Yan, X.-J. Wang and Y. Zhao, *J. Org. Chem.*, 2012, **77**, 10168-10175; (f) M. Suresh, A. K. Mandal, M. K. Kesharwani, N. N. Adarsh, B. Ganguly, R. K. Kanaparthi, A. Samanta and A. Das, *J. Org. Chem.*, 2011, **76**, 138-144; (g) G. T. Spence, C. Chan, F. Szemes and P. D. Beer, *Dalton Trans.*, 2012, **41**, 13474-13485; (h) C. G. Collins, E. M. Peck, P. J. Kramer and B. D. Smith, *Chem. Sci.*, 2013, **4**, 2557-2563; (i) X. Chi, M. Xue, Y. Yao and F. Huang, *Org. Lett.*, 2013, **15**, 4722-4725; (j) L. Cera and C. A. Schalley, *Chem. Sci.*, 2014, **5**, 2560-2567; (k) M. Zhang, X. Yan, F. Huang, Z. Niu and H. W. Gibson, *Acc. Chem. Res.*, 2014, **47**, 1995-2005; (l) A. K. Mandal, M. Gangopadhyay and A. Das, *Chem. Soc. Rev.*, 2015, **44**, 663-676; (m) G. T. Spence, G. V. Hartland and B. D. Smith, *Chem. Sci.*, 2013, **4**, 4240-4244. (n) Y. Kim, Y. H. Ko, M. Jung, N. Selvapalam and K. Kim*, Photochem. Photobiol. Sci.*, 2011, **10**, 1415-1419; (o) I. Hwang, A. Y. Ziganshina, Y. H. Ko, S. Sakamoto, K. Yamaguchi and K. Kim, *Chem Commun.*, 2009, 416-418; (p) J. W. Lee, I. Hwang, W. S. Jeon, Y. H. Ko, S. Sakamoto, K. Yamaguchi and and K. Kim, *Chem. Asian. J.*, 2008, **3**, 1277-1283; (q) J. del Barrio, P. N. Horton, D. Lairez, G. O. Lloyd, C. Toprakcioglu and O. A. Scherman, *J. Am. Chem. Soc.*, 2013, **135**, 11760-11763; (r) F. Tian, D. Jiao, F. Biedermann and O. A. Scherman, *Nat.Commun.*, 2012, **3**,1207.

30   C. Gimenez-Lopez Mdel, M. T. Räisänen, T. W. Chamberlain, U. Weber, M. Lebedeva,

G. A. Rance, G. A. Briggs, D. Pettifor, V. Burlakov, M. Buck and A. N. Khlobystov,

Langmuir, 2011, **27**, 10977-10985.

31   SMART/SAINT; Bruker AXS, Inc.: Madison, WI, 2004.

32   G. M. Sheldrick, SHELXL-2013; University of Göttingen: Göttingen, Germany, 2014.

33   L. J. Farrugia, *J. Appl. Crystallogr.*, 2012, **45**, 849-854. L. J. Farrugia, WinGX, version

2013.3; Department of Chemistry, University of Glasgow: Glasgow, Scotland, 2013.

34   G. M. Sheldrick, SADABS; University of Göttingen, Göttingen, Germany, 1999.

35   (a) A. D. Becke, *J. Chem. Phys.*, 1993, **98**, 5648-5652; (b) A. D. Becke, *Phys. Rev. A*,

1988, **38**, 3098-3100; (c) C. Lee, W. Yang and R. G. Parr, *Phys. Rev. B*, 1988, **37**, 785-

789.

36   *Gaussian 09*, Revision A.02, M. J. Frisch, G. W. Trucks, H. B. Schlegel, G. E. Scuseria,

M. A. Robb, J. R. Cheeseman, G. Scalmani, V. Barone, B. Mennucci, G. A. Petersson, H.

Nakatsuji, M. Caricato, X. Li, H. P. Hratchian, A. F. Izmaylov, J. Bloino, G. Zheng, J. L.

Sonnenberg, M. Hada, M. Ehara, K. Toyota, R. Fukuda, J. Hasegawa, M. Ishida, T.

Nakajima, Y. Honda, O. Kitao, H. Nakai, T. Vreven, J. A. Montgomery, Jr., J. E. Peralta,

F. Ogliaro, M. Bearpark, J. J. Heyd, E. Brothers, K. N. Kudin, V. N. Staroverov, R.

Kobayashi, J. Normand, K. Raghavachari, A. Rendell, J. C. Burant, S. S. Iyengar, J. Tomasi, M. Cossi, N. Rega, J. M. Millam, M. Klene, J. E. Knox, J. B. Cross, V. Bakken, C. Adamo, J. Jaramillo, R. Gomperts, R. E. Stratmann, O. Yazyev, A. J. Austin, R. Cammi, C. Pomelli, J. W. Ochterski, R. L. Martin, K. Morokuma, V. G. Zakrzewski, G. A. Voth, P. Salvador, J. J. Dannenberg, S. Dapprich, A. D. Daniels, O. Farkas, J. B. Foresman, J. V. Ortiz, J. Cioslowski and D. J. Fox, Gaussian, Inc., Wallingford CT, 2009.

TOC

Amino-ether macrocycle that forms Cu^{II} templated threaded heteroleptic complexes: A detailed selectivity, structural and theoretical investigations

Saikat Santra, Sandip Mukherjee, Somnath Bej, Subrata Saha and Pradyut Ghosh*

Department of Inorganic Chemistry, Indian Association for the Cultivation of Science, 2A & 2B

Raja S. C. Mullick Road, Kolkata 700032, India. E-mail: icpg@iacs.res.in
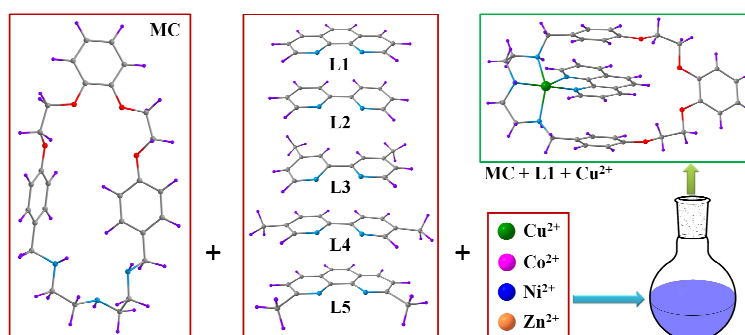
Self-sorting behavior of a newly synthesized macrocycle with divalent metal ions and aromatic ligands via pseudorotaxane formation has been described.